

## TRAVELLING MAGNETIC FIELD MIXING FOR PARTICLE DISPERSION IN LIQUID METAL

*V. Bojarevics<sup>1</sup>, K. Pericleous<sup>1</sup>, M. Garrido<sup>2</sup>,  
Y. Fautrelle<sup>2</sup>, L. Davoust<sup>2</sup>*

<sup>1</sup> *University of Greenwich, Park Row, London, SE10 9LS, UK*

<sup>2</sup> *SIMAP-EPM. BP 75, 38402 Saint Martin d'Hères, France*

The experimental Bridgman type furnace combined with travelling magnetic field Bitter coil mixing arrangement is applied to investigate the solidification structure and the additive particle distribution dynamics. Supporting numerical models combine the time dependent electromagnetic field, developing turbulent flow, moving free surface and solidification front with the Lagrangian dynamic particle tracking. The results demonstrate that the mixing flow direction has direct impact on the particle concentration in the final solidified sample.

**Introduction.** In order to enhance the mechanical properties of solidified metallic material, the transition from columnar to equiaxed grains should be promoted and the grain size reduced. For this purpose, the use of inoculants such as TiB<sub>2</sub> microparticles as grain refiners is very efficient [1–3]. The introduction and distribution of the micro size particles inside the material represents always a challenge, especially when the particle size is decreased. Different methods have been developed such as mechanical stirring, pulse magnetic fields or ultrasound. The advantage of using magnetic fields is the completely contactless influence on the liquid metal. In the case of a travelling magnetic field (TMF), the flow direction and its intensity can be easily controlled to produce required distribution of the inoculant particles within the matrix material. The TMF can be used to increase the number of nucleation points which will enhance the reduction of the grain size in the alloy [3, 4] and to homogenize the temperature of the melt. The electromagnetic mixing helps to produce equiaxed dendrites and prevent the growth of cellular dendrites [5, 6].

Melting light metal alloys (Al, Mg, etc.) in the presence of electromagnetic (EM) field can help to diffuse inclusions of various sizes in the liquid volume or, oppositely, to concentrate these on the surface of the solidified melt. Barnard *et al.* [7] demonstrated experimentally that melting in a high frequency AC field indeed brings particles to selected locations on the surface of a consequently solidified metallic sample. Bubbles and inclusions were observed to move selectively in the presence of EM field during the steel casting [8]. Materials of special properties, like an increased concentration of additive particles near the surface, are produced in the presence of the imposed electromagnetic field [9].

Numerically the particle paths in the stirred liquid metal can be predicted accounting for the added electromagnetic force effects [10, 11]. The electromagnetic force acts directly only on electrically conducting inclusions, however, the electromagnetic force in the surrounding fluid creates a gradient of pressure giving an additional integral force even on the non-conducting inclusions of various sizes and composition [12]. The gravity induced buoyancy acts vertically, while the EM ‘buoyancy’ acts in the direction opposite to the EM force. In addition to this, the large scale electromagnetically driven flow circulation exerts a drag force, torque and shear, which contribute to the particulate transport. The paper presents re-

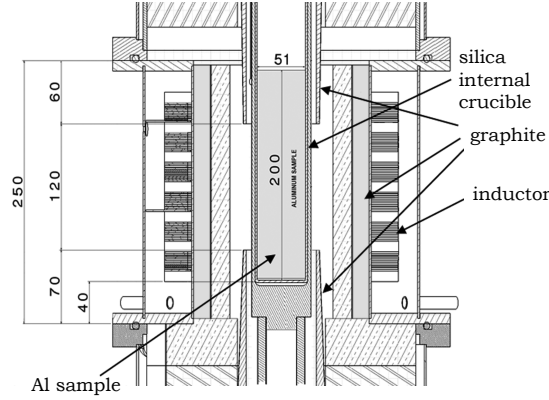


*Fig. 1.* The crucible and furnace dimensions in cross-section of the experimental device with a Bitter coil at SIMAP, Grenoble.

sults obtained using a TMF of low intensity during the melting of aluminum alloy 357 with  $\text{TiB}_2$  microparticles added with the purpose of grain refining.

**1. Experimental procedures.** Experiments were carried out using a Bridgman furnace equipped with a Bitter coil (Fig. 1). The furnace VB2 (Vertical Bridgman 2 inches) manufactured by Cybestar is characterized by a zone of a controlled temperature gradient. The hot and cold end zones are equipped with graphite resistors for heating. This Bitter coil provides a travelling magnetic field of 10 mT and frequency of 50 Hz. The phase shift is set as 60 degrees between the coil sections.

The material used as a matrix material was Aluminum 357. This alloy is commonly used in casting of aerospace structures.  $\text{TiB}_2$  microparticles were selected to be mixed with aluminum 357. The diameter of the particles was  $8.6\mu\text{m}$  and its density  $4.52\text{ g/cm}^3$ . The percentage in weight added to the aluminum alloy was 0.85%. The final weight of the specimen was 730 g. The material is introduced in the furnace inside a crucible made of quartz which is supported by a graphite container. Microparticles and aluminium are introduced at the same time in the furnace. A block of the filling material was made using a stack of the plates filled with the  $\text{TiB}_2$  microparticles. The amount of material of the specified weight permits to obtain a final specimen 15 cm high and 5 cm in diameter.

The aluminum alloy has a very high reactivity with oxygen and forms aluminum oxide in milliseconds. In order to avoid an oxide layer over the surface of the crucible, the furnace is subjected to vacuum conditions of  $10^{-6}$  bar at the beginning of the experiment. After this, an open cycle of argon flow of 2.31/min is maintained during the totality of the experiment. The argon pressure inside the furnace is maintained in this way at 1.2 bar.

The aluminum alloy was heated to a temperature of  $800^\circ\text{C}$  imposed in upper and lower resistors. This temperature was maintained during 1.5 hours. Electromagnetic stirring started when this temperature was attained. The upwards and downwards TMF was alternated every 10 minutes and set to upwards direction during the cooling period until the solidification of the material. The temperature of the lower resistor was brought to  $700^\circ\text{C}$  creating a gradient of  $660\text{ K/m}$  which was kept until the end of the cooling. The rapid cooling would enhance the reduction of the grain size, therefore, the cooling rate selected was  $0.25\text{ K/s}$ .

**2. The mathematical model and results.** The mathematical basis of the present model is the time-dependent Navier-Stokes and continuity equations for

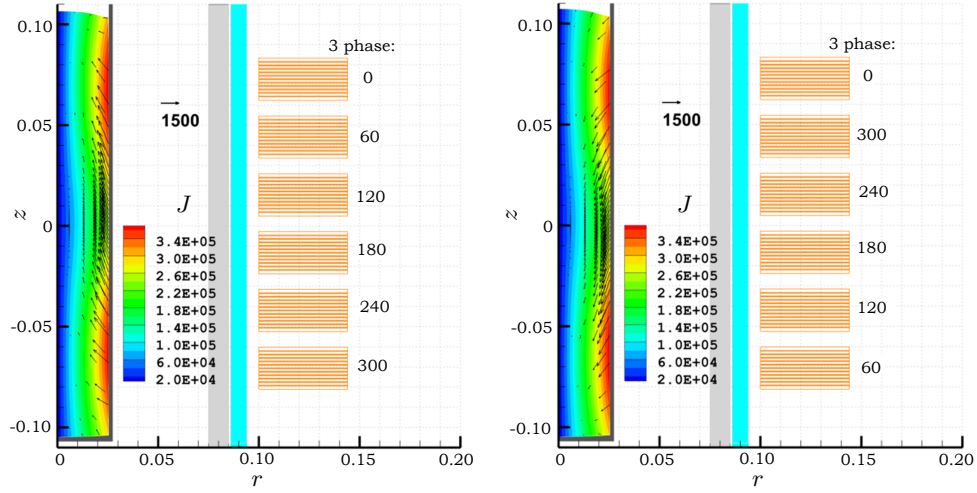


Fig. 2. The TMF induced electric current and force distribution in the aluminium sample for the 300 A effective current value at 50 Hz: (left) directed upwards and (right) downwards by arranging the 3 phase power supply in the Bitter type coil, respectively.

an incompressible fluid and the thermal energy conservation equations with the Joule heating term for the fluid and solid zones of the metal charge [13]. As the typical Reynolds number for the flow considered is about 10000, the turbulent viscosity and the effective thermal diffusivity is the subject of the turbulence model accounting for the EM effects [16, 17] which was validated by direct comparison to the experimentally measured turbulent velocity field in [19]. The numerical solution of the coupled problem is obtained using the pseudo-spectral collocation method, employing the continuous co-ordinate transformation for the free surface and the solidification front shape tracking, as described in the previous publications [16, 18]. The time-dependent fluid flow problem is set with appropriate boundary conditions: at the free surface of the liquid the normal hydrodynamic stress is compensated by the surface tension, whilst at the solid walls the no-slip condition is applied to the velocity wherever there is a contact at any given time. The free surface contact position moves as determined by the force balance and the kinematic conditions. During the melting or solidification, the solid-liquid interface is traced automatically as the solidus temperature surface  $T = T_S$  moves with the coupled effects of the solid fraction-modified specific heat function. The temperature field corresponds to the thermally insulating side wall and the linearly decreasing in time hot top-cold bottom condition. The EM mixing and the passive additive particle distribution (of relatively low concentration, not affecting the fluid material properties) is investigated using the numerical models combining the time dependent EM fields, developing flow fields, the moving free surface and solidification front.

The EM mixing is achieved by the Bitter type coil arranged in separate sections with a prescribed phase shift. The device schematic is shown in Fig. 1 and the numerical model with a computed initial velocity field in Fig. 3.

The AC phase shift permits to create the travelling magnetic field either upward or downward (Fig. 2 shows the time average EM force distribution), which permits a variety of the mixing patterns affecting the solidification front and various scenarios of the particle motion. Fig. 4 demonstrates the shape of the solidification front and the velocity pattern for the upward and downward TMF cases

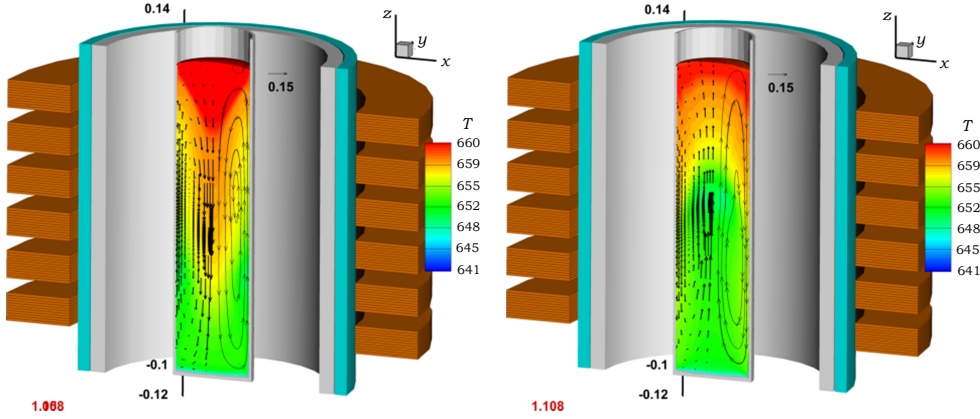


Fig. 3. The initial velocity field in liquid metal due to the upward (left) and downward (right) TMF before the solidification is started.

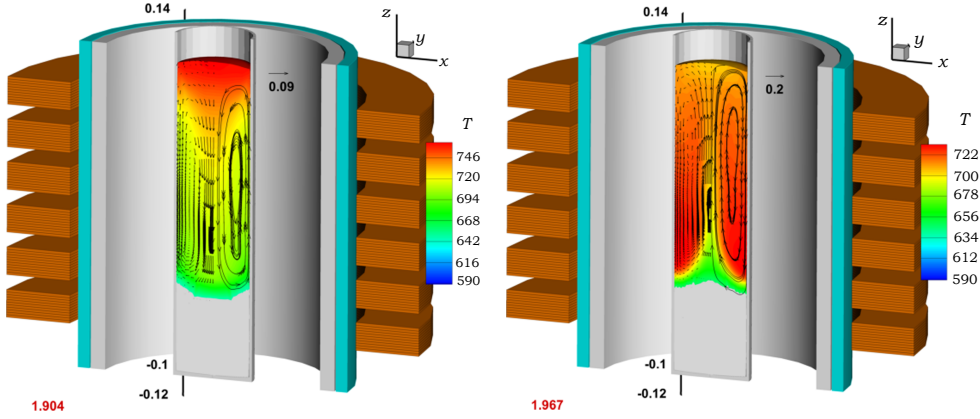


Fig. 4. The velocity field in aluminium samples due to the upward (left) and downward (right) TMF during the development of the solidification front.

after a long time numerical simulation. The concave solidification front shape developed with the upward TMF is thought to be more beneficial to avoid particle cluster (larger particles in our simulation) collection in the bulk of the solidified metal. This recommendation was used in the experiment with the added  $\text{TiB}_2$  particles in the aluminium melt.

The particles of micro to nano-size can be added at desired locations in order to follow their paths and concentration (a relatively low concentration, not affecting the fluid material properties), following their distribution in the gradually solidified metal ingot. Larger particles ( $>10\text{ }\mu\text{m}$ ) are the most sensitive to the buoyancy and EM force effects [11, 12, 14, 15], while smaller size particles follow closely the fluid flow pattern, only deviating in the regions of the higher EM force density and being entrapped when reaching the solidification front. The choice of flow pattern ensures the desired distribution of the particles. The upward EM field favors the fast entrapment of the particles at the bottom solidification front (Fig. 5, left). On the contrary, the downward travelling field creates the flow shown in the right of Fig. 4, which leads to enhanced particle concentration at the top part of the melt (Fig. 5, right), thus delaying or even preventing the additive supply to the solidification front.

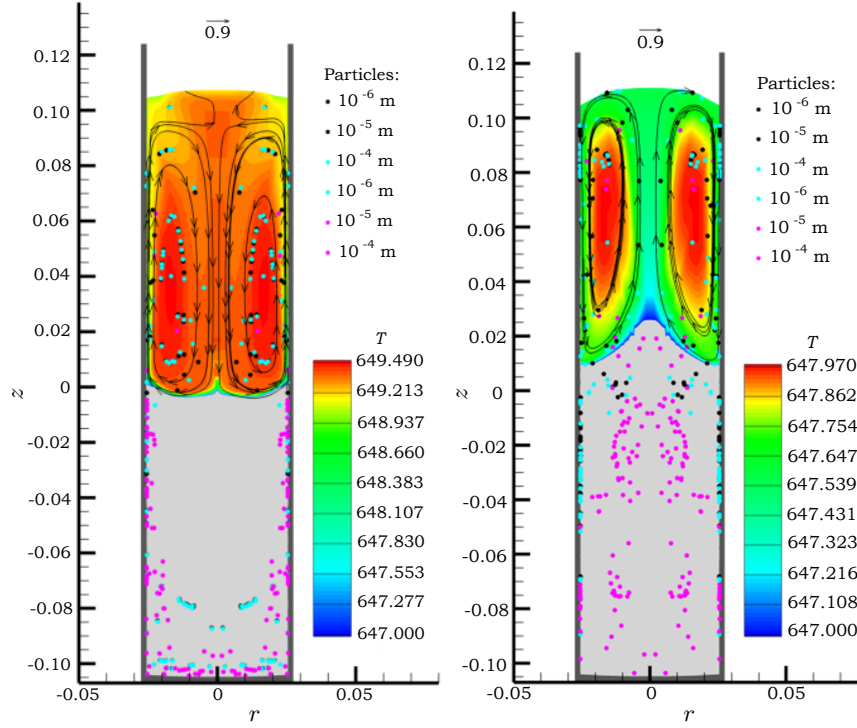


Fig. 5. Various size  $\text{TiB}_2$  particle trajectories in aluminium melt for the upward (left) and the downward (right) TMF.

The results presented are preliminary and a full experimental verification is expected. The numerical model indicates areas in which the magnetic field is the most effective and facilitates to choose the optimum flow direction for the particle dispersion to the solidified metal matrix. The highest intensity of the magnetic field is located at the middle of the Bitter coil area. In consequence, the particles would be more effectively dispersed if they were positioned in the mid-level location at the start of the experiment.

**3. Experimental results and discussion.** The microscopic study of the solidified specimens revealed an apparently good dispersion of the particles. Agglomeration and settling can easily occur due to the electromagnetic effects of the upward TMF and the difference in density between aluminum and  $\text{TiB}_2$ . The images obtained from the analysis of material from the lower part of the crucible (but some distance away from the bottom) showed no signs of agglomeration. The extraction of the particles could have been the result of the polishing performed on the samples. The upper part of the specimen showed different results. The number of particles found during the optical inspection was higher than on the lower part. Signs of possible  $\text{TiB}_2$  agglomerates were found. The characterization of the specimens is still in process and the number of particles will be determined accurately in the future work. The following images (Fig. 6) were taken from samples of the lower part of the specimen. The images show equiaxial grains at distances of less than 1 cm from the side wall of the crucible. There are clear signs of refining the aluminum 357 stirred with the  $\text{TiB}_2$  additive (Fig. 6, left), compared to the case of the aluminum 357 solidified without refining (right).

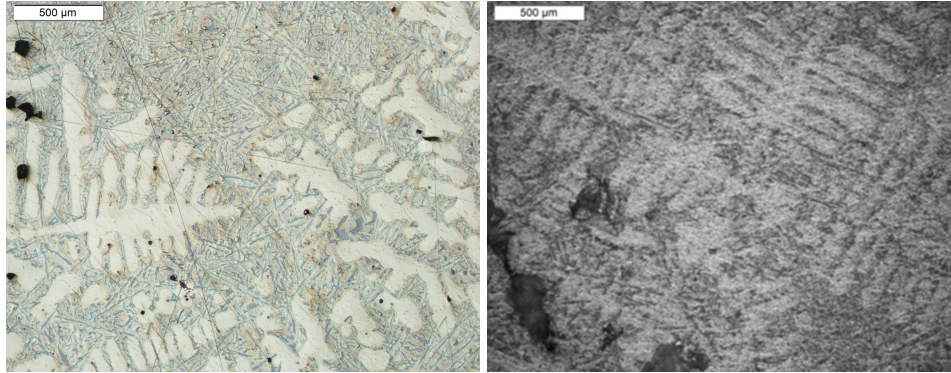


Fig. 6. Micrographs of the solidified samples: (left) aluminum 357 stirred with the  $\text{TiB}_2$  additive; (right) equiaxial dendrites and signs of porosity without refining.

**4. Conclusions.** Intense mixing can be achieved using both the upward and the downward travelling magnetic field. The melt front shape is strongly affected by the flow direction and by the type of side wall thermal conditions. The particle paths and the concentration can be optimized to the desired outcome manipulating the EM field. The combined use of grain refiner and low intensity travelling magnetic field has shown positive results in the refining of the material.

**Acknowledgments.** The authors acknowledge financial support from the ExoMet Project (co-funded by the European Commission (contract FP7-NMP3-LA-2012-280421), by the European Space Agency and by the individual partner organizations).

## REFERENCES

- [1] M. NOWAK, H.B. NADENDLA. Grain refiner for aluminium-silicon sand casting alloys. *Light Metals 2012* (Ed. C.E. Suarez, The Minerals and Materials Society 2012), pp. 349–353.
- [2] A.L. GREER, A.M. BUNN, A. TRONCHE, P.V. EVANS, D.J. BRISTOW. Modelling of inoculation of metallic melts: application to grain refinement of aluminium by  $\text{AlTiB}$ . *Acta Mater*, vol. 48 (2000), pp. 2823–2835.
- [3] D.G. MCCARTNEY. Grain refining of aluminium and its alloys using inoculants. *International Materials Reviews*, vol. 34 (1989), no. 5, pp. 247–260.
- [4] NEW PROCESS FOR GRAIN REFINEMENT OF ALUMINIUM. *Alcoa Report* (Contract No. DE-FC07-98ID13665, September 22, 2000).
- [5] C. VIVES. Hydrodynamic, thermal and crystallographical effects of an electromagnetically driven rotating flow in solidifying aluminium alloys. *Int. J. Heat Mass Transfer*, vol. 33 (1990), pp. 2585–2598.
- [6] J.K. ROPLEKAR, J.A. DANTZIG. A study of solidification with a rotating magnetic field. *Int. J. Cast Metals Res.*, vol. 14 (2001), pp. 79–95.
- [7] L. BARNARD, R.F. BROOKS, P.N. QUESTED AND K.C. MILLS. Evaluation of alloy cleanliness using cold crucible melting. *Ironmaking and Steelmaking*, vol. 20 (1993), no. 5, pp. 344–349.

- [8] J.W. HAVERKORT, T.W.J. PEETERS. Magnetohydrodynamic effects on insulating bubbles and inclusions in the continuous casting of steel. *Metallurgical and Materials Transactions*, vol. 41B (2010), pp. 1240–1246.
- [9] S. TANIGUCHI, A. KIKUCHI. Removal of nonmetallic inclusion from liquid metal by AC-electromagnetic force. *Proc. the 3rd Int. Symp. Electromagn. Proc. Materials, ISIJ* (Nagoya, 2000), 315–320.
- [10] T. TOH, H. YAMAMURA, H. KONDO, M. WAKOH, SH. SHIMASAKI, S. TANIGUCHI. Kinetics evaluation of inclusions removal during levitation melting of steel in cold crucible. *ISIJ International*, vol. 47 (2007), no. 11, pp. 1625–1632.
- [11] V. BOJAREVICS, K. PERICLEOUS AND R. BROOKS. Dynamic model for metal cleanliness evaluation by melting in cold crucible. *Metallurgical and Materials Transactions B*, vol. 40 (2009), no. 3, pp. 328–336.
- [12] D. LEENOV AND A. KOLIN. Theory of Electromagnetophoresis. 1. Magnetohydrodynamic forces experienced by spherical and symmetrically oriented cylindrical particles. *J. Chem. Phys.*, vol. 22 (1954), no. 4, pp. 683–688.
- [13] V. BOJAREVICS, R.A. HARDING, K. PERICLEOUS AND M. WICKINS. The development and validation of a numerical model of an induction skull melting furnace. *Metall. Materials Transactions B*, vol. 35 (2004), pp. 785–803.
- [14] R. CLIFT, J.R. GRACE AND M.E. WEBER. *Bubbles, Drops, and Particles* (Dover Publications, Mineola, New York, 2005) p. 381.
- [15] P.G. TUCKER. Computation of particle and scalar transport for complex geometry turbulent flows. *J. Fluids Eng.*, vol. 123 (2001), pp. 372–381.
- [16] R.A. HARDING, M. WICKINS, G. KEOUGH, K. PERICLEOUS, V. BOJAREVICS. The use of combined DC and AC fields to increase superheat in an induction skull melting furnace. *Proc. 2005 Int. Symp. Liquid Metal Processing and Casting* (Santa Fe, USA, 2005), 201–210.
- [17] O. WIDLUND. *Modelling of Magnetohydrodynamic Turbulence* (Ph.D. Thesis, Royal Institute of Technology, Stockholm, Sweden, 2000).
- [18] V. BOJAREVICS, K. PERICLEOUS AND M. CROSS. Modelling the dynamics of magnetic semi-levitation melting. *Metall. Materials Transactions B*, vol. 31 (2000), pp. 179–189.
- [19] A. BOJAREVICS, V. BOJAREVICS, YU. GELFGAT AND K. PERICLEOUS. Liquid metal turbulent flow dynamics in a cylindrical container with free surface: experiment and numerical analysis. *Magnetohydrodynamics*, vol. 35 (1999), no. 3, pp. 205–222.

Received 27.05.2015